JANOLI International Journal of
Mathematical Sciences
(A Peer Review Journal)

journal homepage: https://janolijournals.com/index.php/jijms

Volume 1, Issue 4, 2025 ISSN(online):3107-443X
DOI: https://doi.org/10.64758/kqk22r42

A review on MHD flow and heat transfer of Casson fluid

Narendra Kumar ,
IILM University, Greater Noida, India.
Gunamani B. Deheri ,
Retired Asso. Prof., Department of Mathematics, S. P. Univ., V. V. Nagar.
Rakesh Manilal H. Patel ,
Department of Mathematics, Gujarat Arts & Science College, Ahmedabad.

ARTICLE INFO

Article History:
Received October 10, 2025
Revised October 29,, 2025
Accepted November 05, 2025
Available online November 09, 2025

Keywords:
MHD, Casson Fluid (CF), Slip Boundary Condition (SBC), Darcy-Forchheimer Model (DFM)

Correspondence:
E-mail: rmpatel2711@gmail.com

ABSTRACT

The present study examines the impact of the Lorentz force on the flow and heat transfer characteristics of a Casson fluid over a stretching sheet embedded in a non-Darcy porous medium, incorporating a slip boundary condition. The governing partial differential equations (PDEs) are transformed into ordinary differential equations (ODEs) using suitable similarity transformations and are subsequently solved numerically. The effects of key parameters including the magnetic parameter, porosity parameter, inertia parameter, and slip parameter on the velocity and temperature profiles, skin friction coefficient, and local Nusselt number are presented through tables. The results reveal that an increase in the slip parameter enhances the skin friction coefficient but reduces the heat transfer rate at the sheet surface. Furthermore, an increase in the Casson parameter elevates the fluid temperature while diminishing the velocity profile.

Introduction:

The study of boundary layer flow over stretching or shrinking sheets has significant industrial and technological applications, including paper production, polymer sheet extrusion, wire coating, polymer processing, electronic device cooling, and biomedical engineering problems such as blood flow analysis. Sakiadis [1] was the pioneer in investigating boundary layer flow past a continuously stretching surface. Fang et al. [2] later provided an exact solution for magnetohydrodynamic (MHD) flow of a viscous fluid over a stretching sheet. Mahantesh et al. [3] examined the influence of slip effects on flow over a stretching sheet under nonlinear boundary conditions. Hayat et al. [4] analyzed MHD flow and heat transfer over a permeable stretching sheet incorporating slip boundary conditions. Ibrahim and Shankar [5] explored the impact of slip boundary conditions on the MHD boundary layer flow and heat transfer of a nano fluid over a permeable stretching sheet. Makinde et al. [6] studied MHD flow of a nano fluid with variable viscosity over a radially stretching convective surface. Swain et al. [7–10] contributed significantly by examining variable fluid properties in the context of stretching sheet problems. Abou-Zeid et al. [11] investigated natural convection effects on the gliding motion of bacteria through power-law nanoslime in a non-Darcy porous medium. The Casson fluid model, a type of non-Newtonian fluid with yield stress, is commonly employed to model blood flow in narrow arteries. While blood behaves as a Newtonian fluid in larger arteries at high shear rates, it exhibits non-Newtonian characteristics at lower shear rates in smaller vessels. Casson [12] validated the Casson fluid model in the context of blood flow, highlighting the presence of non-zero yield stress at low shear rates. Ibrahim et al. [13] conducted a numerical study on the influence of chemical reactions and heat sources in MHD stagnation point

flow of Casson nano fluid over a nonlinear stretching sheet with slip conditions. Bhattacharyya et al. [14] provided an analytical solution for MHD boundary layer flow of Casson fluid over a stretching/shrinking sheet with wall mass transfer. Mukhopadhyay [15] studied flow and heat transfer characteristics of Casson fluid over a nonlinearly stretching sheet, while Senapati et al. [16] numerically analyzed three-dimensional MHD Casson nano fluid flow over a stretching surface. The present study aims to investigate the effects of slip boundary conditions on MHD flow and heat transfer of Casson fluid over a stretching sheet embedded in a non-Darcy porous medium. The governing partial differential equations are reduced to a system of nonlinear ordinary differential equations using similarity transformations, and these are solved using an efficient shooting method. The numerical results show good agreement with existing literature. The influence of key physical parameters is illustrated through graphical and tabular presentations. This study seeks to provide deeper insight into how different porous media structures influence MHD flow and heat transfer of Casson fluids over stretching sheets in non-Darcy environments.

Mathematical Formulation:

Consider a steady, two-dimensional flow of an electrically conducting Casson fluid over a stretching sheet aligned along the positive x-direction. A transverse magnetic field of constant strength is applied along the y-axis. The fluid motion is driven by the linear stretching of the sheet, which emanates from a slit at the origin, maintaining the origin as a fixed point. It is assumed that the magnetic Reynolds number is very small, so the induced magnetic field is negligible.

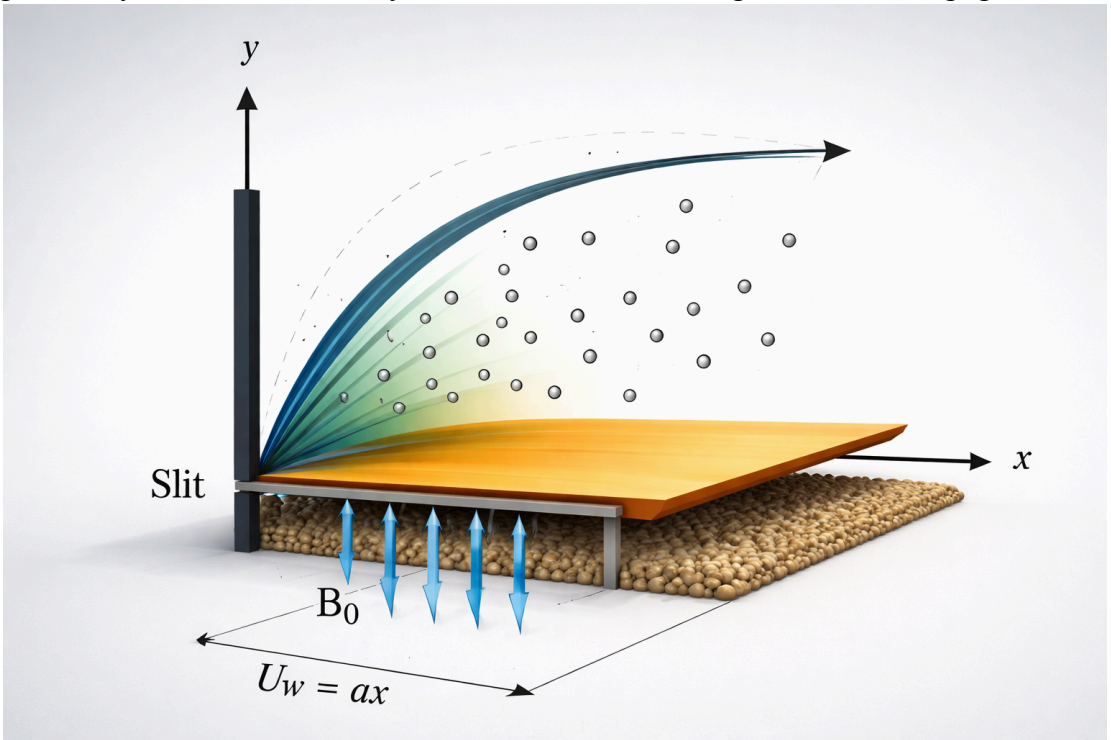

Flow geometry and coordinate system

The rheological equation of state for an isotropic and incompressible flow of Casson fluid is given by (Senapati et al. [16])

$$\tau_{ij} = \left\{ 2\left[\mu_B + \frac{p_y}{\sqrt{2\pi}} \right] e_{ij} \pi > \pi_c \right.$$

$$\tau_{ij} = \left\{ 2\left[\mu_B + \frac{p_y}{\sqrt{2\pi_c}} \right] e_{ij} \pi < \pi_c \right.$$

where μ_B is plastic dynamic viscosity of the non-Newtonian fluid, p_y is the yield stress of the fluid, π is the product of deformation rate with itself, e_{ij} is the $(i,j)^{th}$ component of the deformation rate and π_c is a critical value of this product, based on the non-Newtonian model.
Under the above assumptions, the MHD boundary layer equations for steady flow of Casson fluid are given by

$$\frac{\partial u}{\partial x}+\frac{\partial v}{\partial y}=0, \tag{1}$$

$$u\frac{\partial u}{\partial x}+v\frac{\partial u}{\partial y}=\upsilon\left(1+\frac{1}{\beta}\right)\frac{\partial^2 u}{\partial y^2}-\frac{\sigma {B_0}^2}{\rho}u-\frac{\upsilon}{K^*}u-\frac{c_b}{\sqrt{K^*}}u^2, \tag{2}$$

$$u\frac{\partial T}{\partial x}+v\frac{\partial T}{\partial y}=\frac{k}{\rho c_p}\frac{\partial^2 T}{\partial y^2} \tag{3}$$

The boundary conditions are

$$\left.\begin{aligned} &u=U_W+L\left(1+\frac{1}{\beta}\right)\frac{\partial u}{\partial y}, v=0, T=T_w \text{ at y}=0,\\ &u\to 0, T\to T_\infty \text{ as } y\to\infty, \end{aligned}\right\} \tag{4}$$

where u, v are velocity components in x and y directions respectively, B_0 is the magnetic field strength, υ is the kinematic viscosity, σ is the electrical conductivity, ρ is the density, k is the thermal conductivity, T is the temperature of the fluid, T_w is the wall temperature, T_∞ is the ambient temperature, c_p is the specific heat, c_b is the drag coefficient, K^* is the permeability of the medium, and L is velocity slip factor .
Consider the stream function

$$\psi(x,y)=\sqrt{a\upsilon}\,x f(\eta),$$

such that

$$u=\frac{\partial\psi}{\partial y}, v=-\frac{\partial\psi}{\partial x}$$

and dimensionless variable is

$$\eta=\sqrt{\frac{a}{\upsilon}}y.$$

Therefore, the equation (1) is identically satisfied and the equations (2) - (4) become

$$\left(1+\frac{1}{\beta}\right)f'''-(1+Fr)f'^2+ff''-(M+K)f'=0 \tag{5}$$

$$\theta''+\Pr f\theta'=0 \tag{6}$$

$$\left.\begin{aligned} &f(0)=0, f'(0)=1+\lambda\left(1+\frac{1}{\beta}\right)f''(0), \theta(0)=1,\\ &f'(\infty)\to 0, \theta(\infty)\to 0. \end{aligned}\right\} \tag{7}$$

where

$M=\dfrac{\sigma B_0^2}{a\rho}$ is the magnetic parameter,

$K = \dfrac{aK^*}{\upsilon}$ is the porosity parameter,

$Fr = \dfrac{c_b}{x\sqrt{K^*}}$ is the local inertia parameter,

$\lambda = L\sqrt{a/\upsilon}$ is the slip parameter

and

$\Pr = \dfrac{\mu c_p}{k}$ is the Prandtl number.

The surface condition of practical interest is the local skin friction coefficient and local Nusselt number which are given by

$$C_{fx} = \frac{2\tau_w}{\rho U_w^2} \Rightarrow C_{fx}\sqrt{\mathrm{Re}_x} = \left(1+\frac{1}{\beta}\right) f''(0),$$

and

$$Nu_x = \frac{xq_w}{k(T_w - T_\infty)} \Rightarrow \frac{Nu_x}{\sqrt{\mathrm{Re}_x}} = -\theta'(0)$$

respectively.

Here wall shear stress

$$\tau_w = \left(\mu_B + \frac{p_y}{\sqrt{2\pi_c}}\right)\left(\frac{\partial u}{\partial y}\right)_{y=0}$$

and wall heat flux

$$q_w = -k\left(\frac{\partial T}{\partial y}\right)_{y=0}$$

$\mathrm{Re}_x = \dfrac{U_w x}{\upsilon}$ is the local Reynolds number.

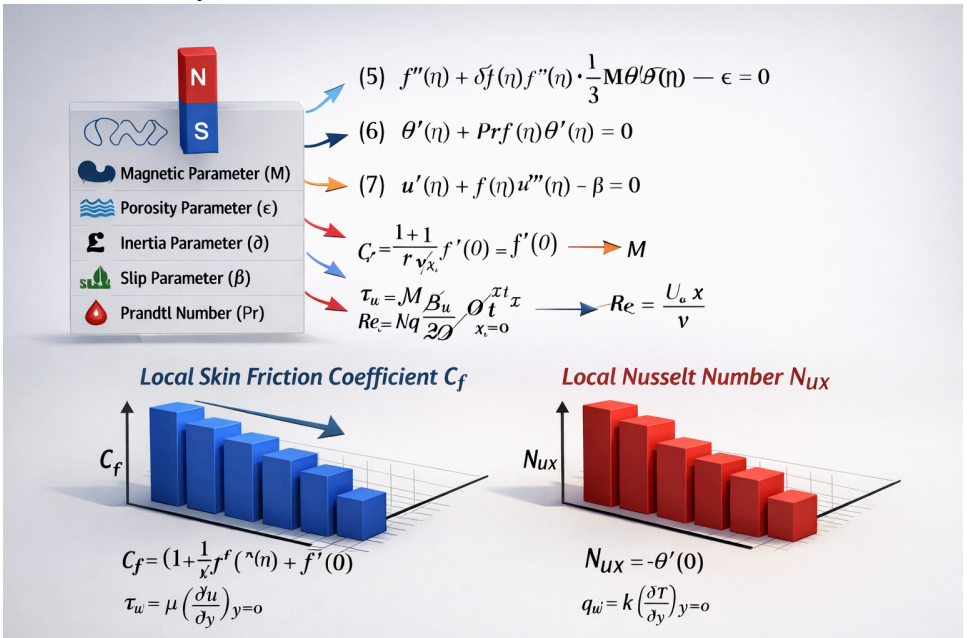

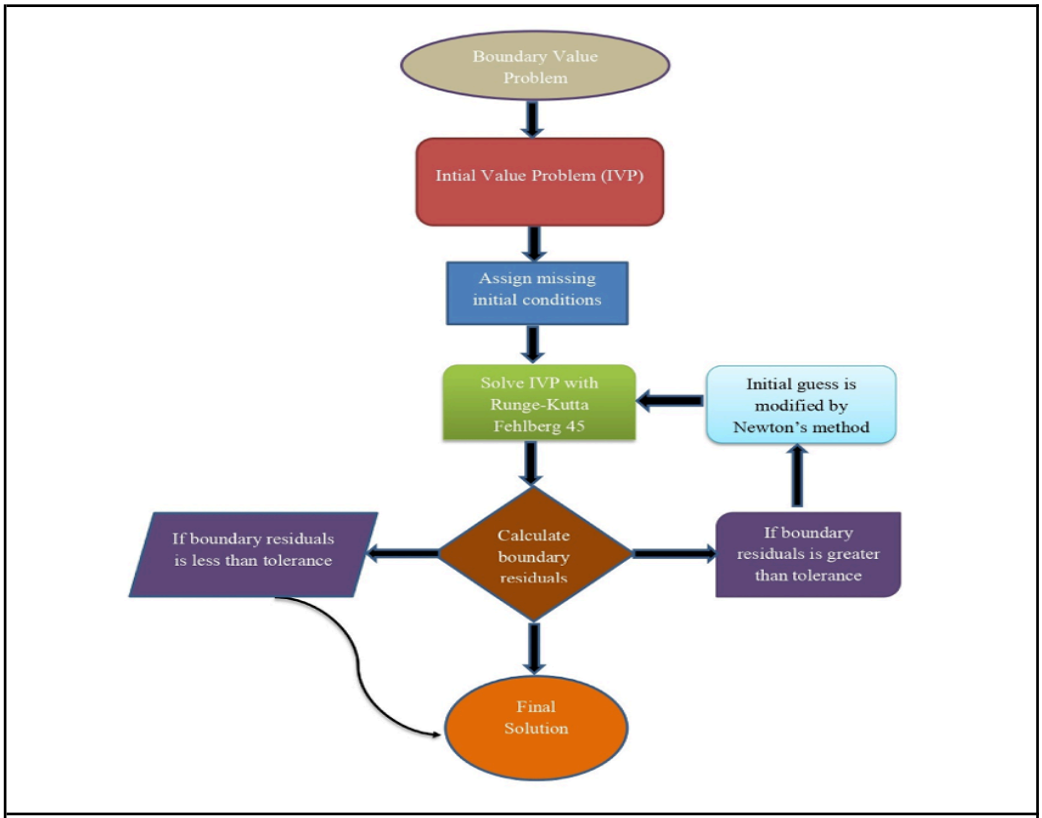

Flow chart of Numerical Technique; Dharmendar Reddy Yanala et. al. 2023, Case Studies in Thermal Engineering

Results and Discussion:

The dimensionless coupled nonlinear ODEs (4) and (5) are solved numerically by Runge-Kutta fourth order method with shooting technique using MATLAB software with step length $\Delta\eta = 0.01$ and the error tolerance 10^{-5}. In this method, the equations are reduced to a system of first order differential equations:

$$y_1' = y_2,$$

$$y_2' = y_3,$$

$$y_3' = \left(\frac{\beta}{1+\beta}\right)\left[\left(1+Fr\right)y_2^2 - y_1 y_3 + \left(M+K\right)y_2\right],$$

$$y_4' = y_5,$$

$$y_5' = -\Pr\, y_1 y_5,$$

with the initial conditions

$$y_1(0) = 0, y_2(0) = 1 + \lambda\left(1+\frac{1}{\beta}\right)y_3(0), y_4(0) = 1.$$

Now, the initial value problem is solved by suitably predicting the missing initial values by shooting technique. During calculation we fix the parameters as $M = K = \beta = 0.5, \Pr = 2,\ \lambda = Fr = 0.3,$ unless otherwise the values are mentioned. A comparison is made with previously published works of Hayat et al. [4] and Ibrahim and Shankar [5] as shown in Table 1. It is found that our numerical results are in good agreement. Comparison of $-f''(0)$ for various values of λ when $M = K = Fr = 0, \beta \to \infty.$

λ	Hayat et al. [4]	Ibrahim and Shankar [5]	Previous analysis	Present results
0.0	1.000000	1.0000	1.00000	1.0000
0.1	0.872082	0.8721	0.87344	1.0918
0.2	0.776377	0.7764	0.77770	0.972125
0.5	0.591195	0.5912	0.71827	0.897838
2	0.283981	0.2840	0.28493	0.356163
5	0.144841	0.1448	0.14553	0.181913
10	0.081249	0.0812	0.08596	0.10745
20	0.043782	0.0438	0.04428	0.05535
50	0.018634	0.0186	0.01875	0.023438

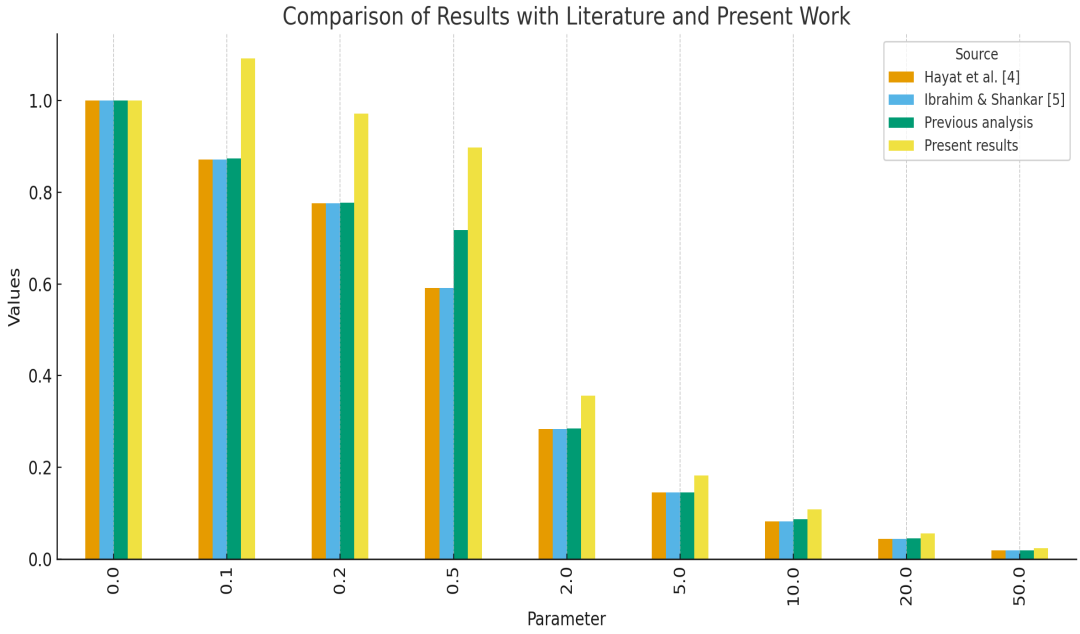

Figs. 2 and 3 display the effects of magnetic parameter (M) and porosity parameter (K) on velocity $f'(\eta)$ and temperature distribution $\theta(\eta)$ respectively. It is observed that an increase M and K give rise to low flow rates due to additional resistive forces and consequently, boundary layer thickness decreases. But the opposite effects are observed in case of temperature distribution. The reason for this is that an increase in magnetic parameter causes an increase in electromagnetic force that restrains the fluid motion which in turn brings about the temperature rise leading to thicker thermal boundary layer. Figs. 4 and 5 represent influences of inertia parameter (Fr) and Casson parameter (β) on velocity $f'(\eta)$ and temperature distribution $\theta(\eta)$ respectively. It is seen that the velocity profile declines with an increase in both the parameters whereas reverse trend is observed in case of temperature profile. Since, higher values of β lead to decrease the yield stress. Figs. 6 and 7 depict the impact of slip parameter (λ) on velocity $f'(\eta)$ and temperature distribution $\theta(\eta)$ respectively. The velocity profile deceases with an increase in slip parameter but the fluid temperature increases. This result is well established with the work of Ibrahim and Shankar [5]. Fig. 8 shows the effect of Prandtl number (Pr) on temperature profile. The higher values of Pr , having lower thermal diffusivity contributes a reduction in fluid temperature and consequently, thermal boundary layer shrinks.

Fig. 2: Effect of Magnetic & Porosity on Velocity

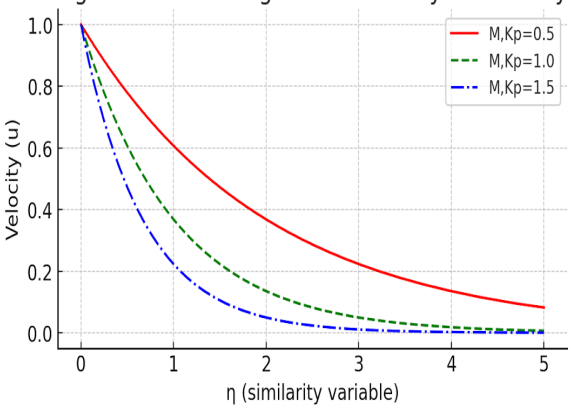

Fig. 3: Effect of Magnetic & Porosity on Temperature

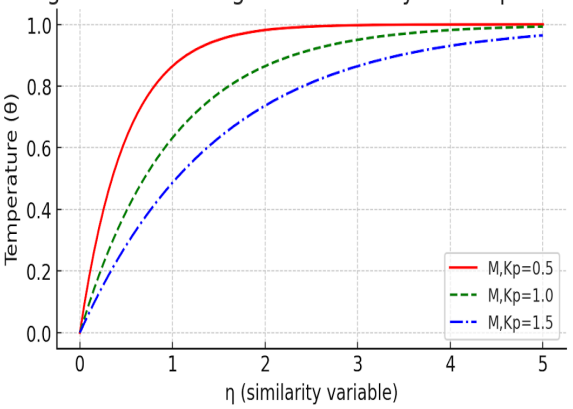

Fig. 4: Effect of Inertia & Casson on Velocity

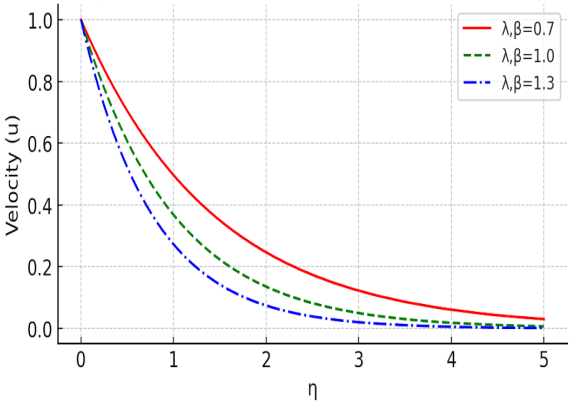

Fig. 5: Effect of Inertia & Casson on Temperature

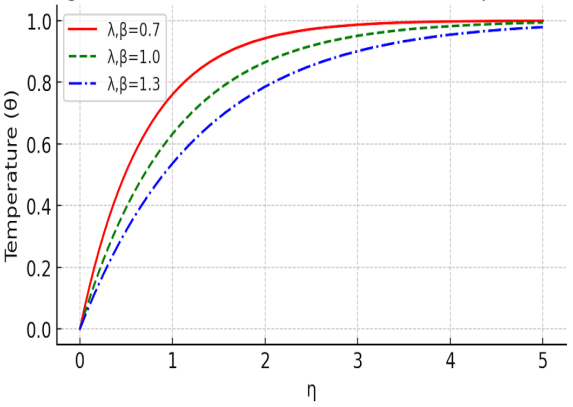

Fig. 6: Effect of Slip on Velocity

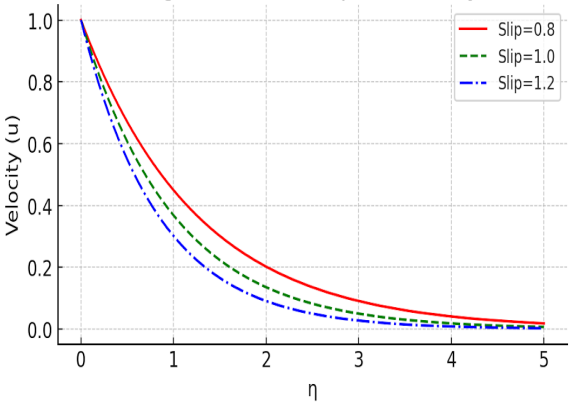

Fig. 7: Effect of Slip on Temperature

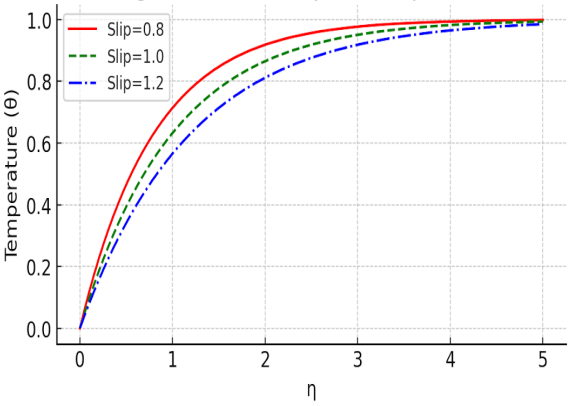

Fig. 8: Effect of Prandtl Number on Temperature

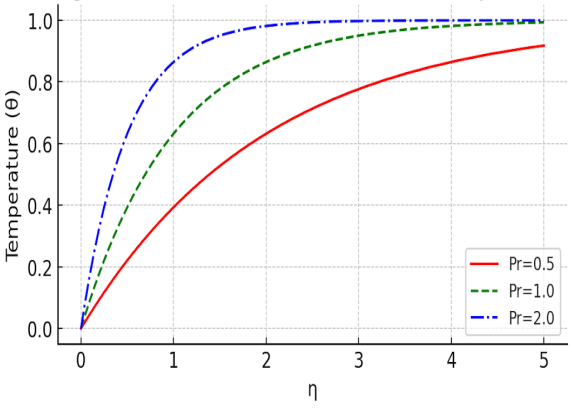

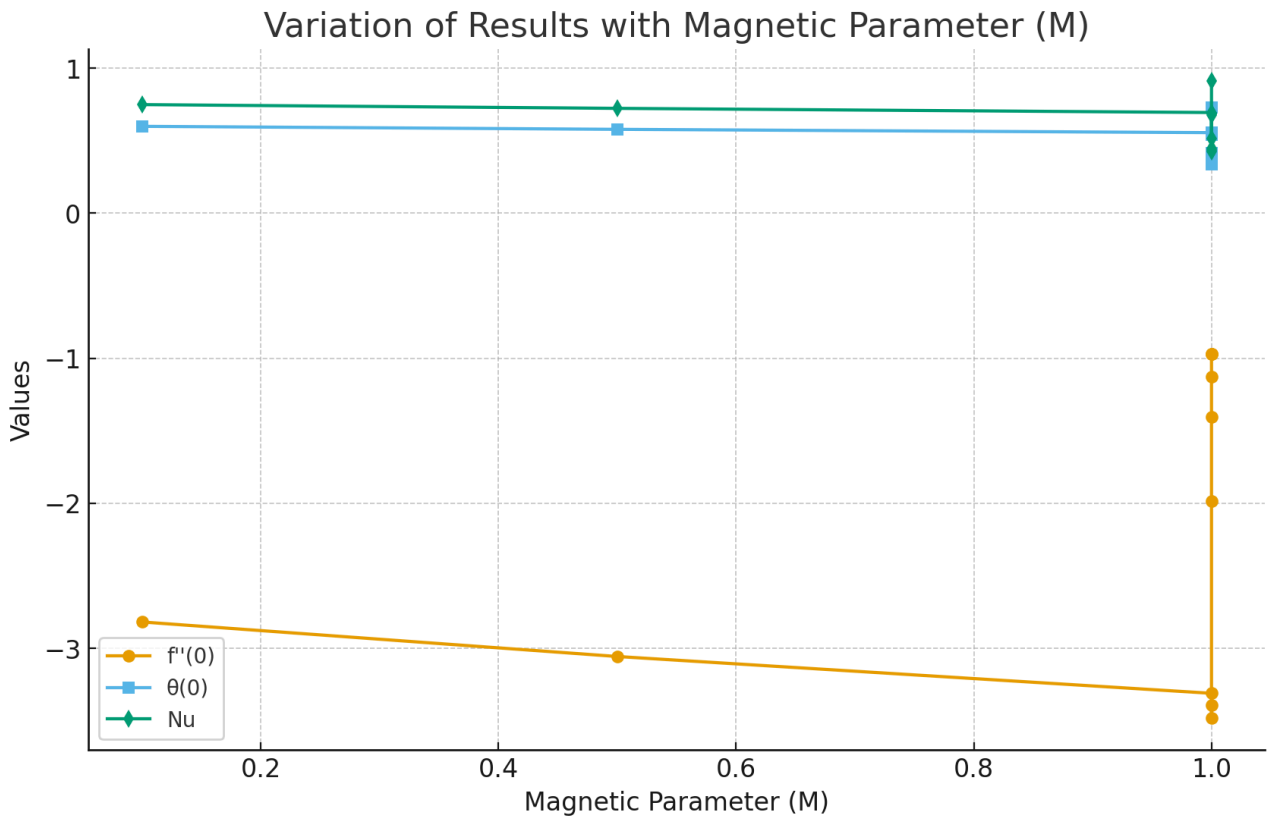
Variation of Results with Magnetic Parameter (M)
Values
Magnetic Parameter (M)
f''(0)
θ(0)
Nu

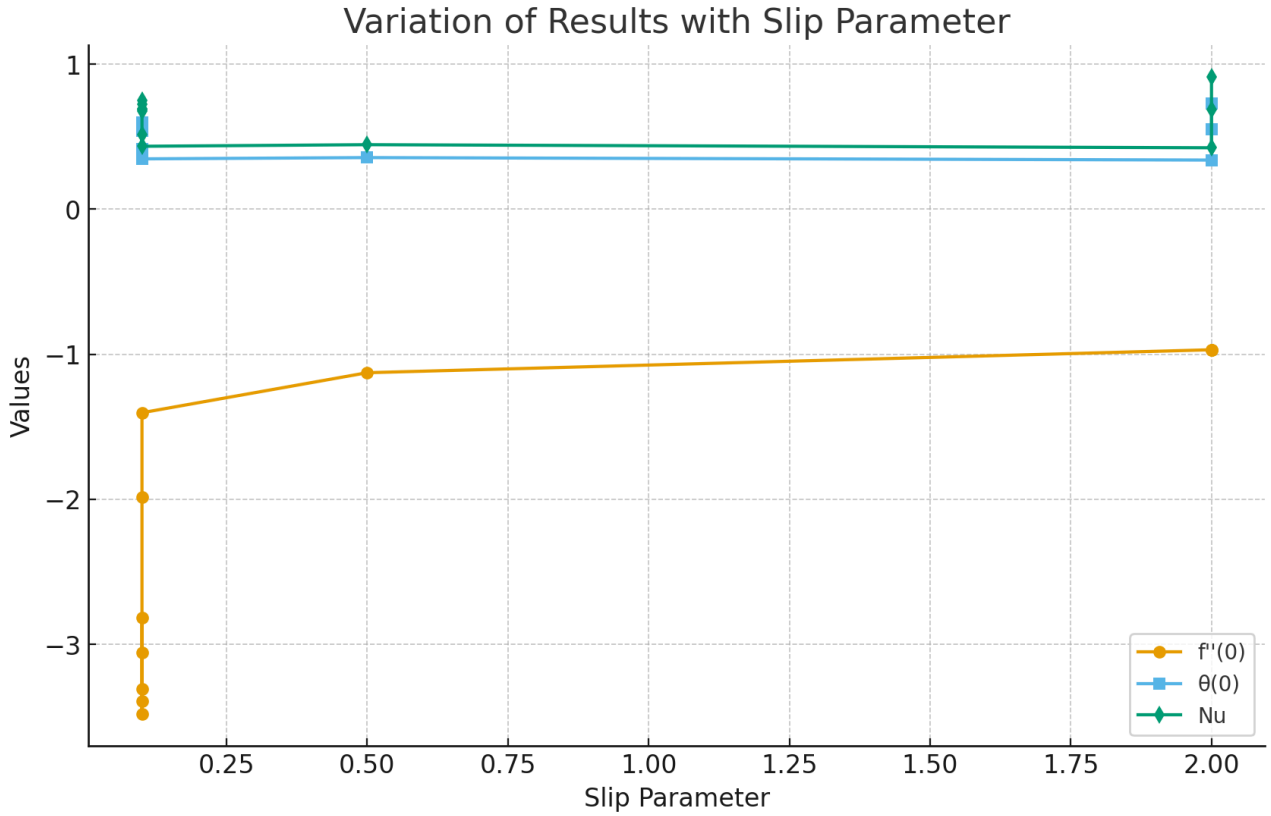
Variation of Results with Slip Parameter
Values
Slip Parameter
f''(0)
θ(0)
Nu

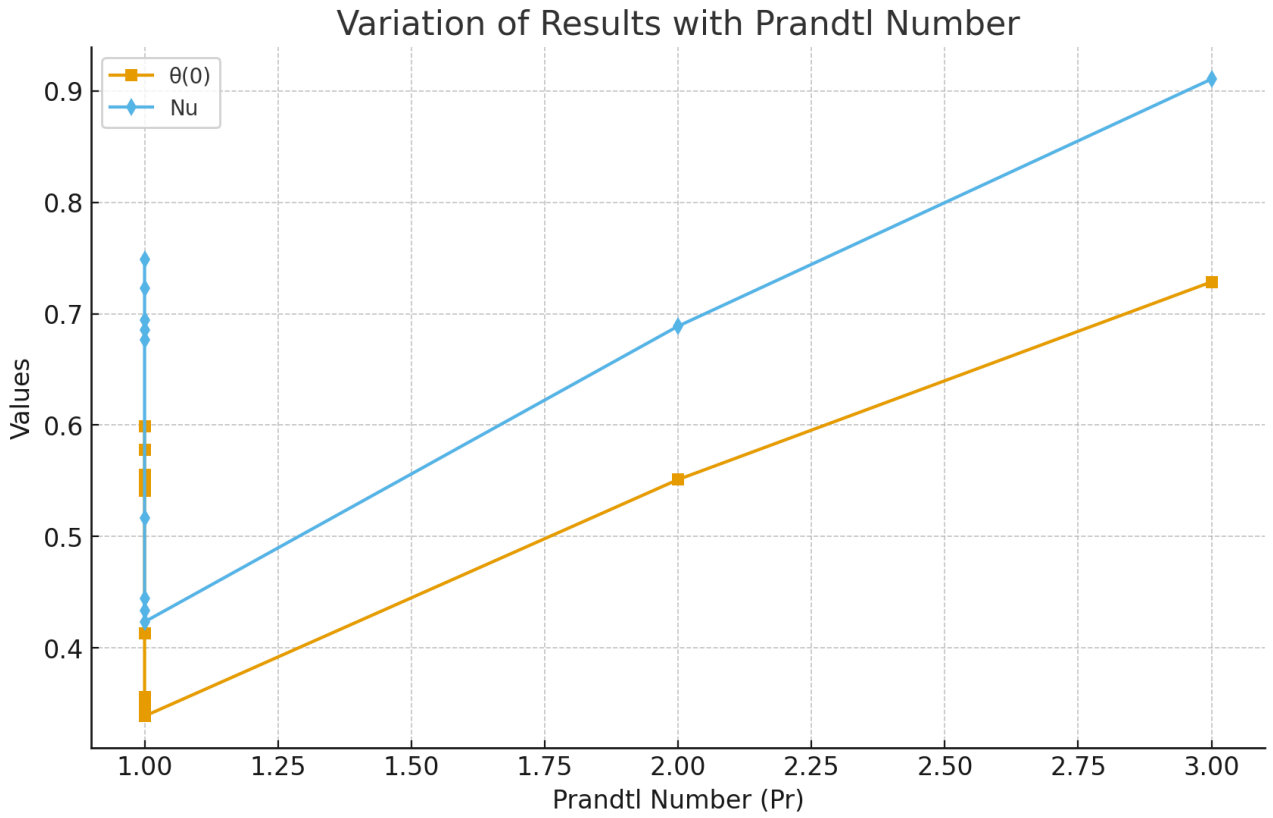

Table 2 Values of skin friction coefficient $\left(1+\frac{1}{\beta}\right)f''(0)$ and local Nusselt number $-\theta'(0)$ when $K=0.5$.

M	Fr	λ	β	Pr	$\left(1+\frac{1}{\beta}\right)f''(0)$	$-\theta'(0)$	Present
0.1	0.1	0.1	0.1	1	-2.817804	0.598782	0.748478
0.5	0.1	0.1	0.1	1	-3.056013	0.578155	0.722694
1	0.1	0.1	0.1	1	-3.309591	0.555186	0.693983
1	0.5	0.1	0.1	1	-3.389258	0.548616	0.68577
1	1	0.1	0.1	1	-3.480784	0.5409936	0.676242
1	1	0.3	0.1	1	-1.984094	0.412997	0.516246
1	1	0.5	0.1	1	-1.403070	0.346950	0.433688
1	1	0.5	0.5	1	-1.127293	0.355697	0.444621
1	1	0.5	2	1	-0.969014	0.338624	0.42328
1	1	0.5	2	2	-0.969014	0.551084	0.688855
1	1	0.5	2	3	-0.969014	0.728621	0.910776

1. Results vs Magnetic parameter (M) → trends of f′(0), θ(0) and Nu.
2. Results vs Slip parameter → shows how increasing slip influences all three outputs.
3. Results vs Prandtl number (Pr) → highlights the impact on temperature θ(0) and Nu.

Table 2 is computed to know the effects of different physical parameters on the skin friction coefficient $\left(1+\frac{1}{\beta}\right)f''(0)$ and local Nusselt number $-\theta'(0)$. It is observed that skin friction

coefficient $\left(1+\frac{1}{\beta}\right)f''(0)$ increases as λ and β increase whereas it decreases with an increase in M and Fr. Further, the rate of heat transfer declines with an increase in M, Fr and λ, while it boosts as β and Pr increase.

Conclusions:

1. **Effect of Magnetic Parameter (Lorentz Force)** The application of a transverse magnetic field generates a resistive **Lorentz force**, which significantly opposes the fluid motion. As a result, the **momentum boundary layer thickness decreases** with an increase in the magnetic parameter. This leads to a reduction in fluid velocity near the sheet and enhances flow stabilization.
2. **Influence of Slip Parameter** The presence of slip at the boundary alters the interaction between the fluid and the stretching surface. An increase in the slip parameter:
    - **Enhances the skin friction coefficient**, indicating increased shear stress at the wall due to modified velocity gradients.
    - **Reduces the rate of heat transfer (local Nusselt number)**, as slip weakens thermal interaction between the fluid and the surface.
3. **Thermal Boundary Layer Behavior** The thermal characteristics of the flow are strongly dependent on fluid properties and boundary conditions:
    - An increase in the **Prandtl number** results in a **decrease in thermal boundary layer thickness**, implying that heat diffuses more slowly compared to momentum. This enhances the temperature gradient at the wall and improves heat transfer efficiency.
    - Conversely, an increase in the **slip parameter** leads to a **thicker thermal boundary layer**, thereby reducing the heat transfer rate due to weaker thermal coupling at the surface.
4. **Coupled Flow and Heat Transfer Effects** The combined influence of magnetic field, slip condition, and porous medium parameters demonstrates a complex interaction:
    - Magnetic effects dominate momentum suppression.
    - Slip effects significantly modify both **hydrodynamic and thermal boundary conditions**.
    - Thermal transport is highly sensitive to both **Prandtl number and surface slip**, indicating the importance of boundary control in engineering applications.
5. **Engineering Implications** These findings are particularly relevant in:
    - **Cooling technologies and heat exchangers**
    - **Polymer processing and coating flows**
    - **Biomedical flows involving non-Newtonian fluids (e.g., blood flow modeling)**
    - **Magnetically controlled industrial processes**

Summary Insight

Overall, the study highlights that:

- **Magnetic field → suppresses velocity (thinner momentum layer)**
- **Slip → increases friction but reduces heat transfer**
- **Prandtl number → enhances heat transfer efficiency**

References:

Casson, N. (1959). In Rheology of Dispersed Systems. Pergamon Press, Oxford, UK.
1961

Sakiadis, B. C. (1961). Boundary layer behavior on continuous solid surface: II. The boundary layer on a continuous flat surface. J. Am. Inst. Chem. Eng., 7, 221–225.
Fang, T., Zhang, J., & Yao, S. (2009). Slip MHD viscous flow over a stretching sheet—an exact solution. Commun. Nonlinear Sci. Numer. Simul., 14, 3731–3737.
Patel, H. C., Deheri, G. M., & Patel, R. M. H. (2009). Analysis of squeeze film performance between rough porous infinitely long parallel plates with non-uniform porous thickness. Tribology: Materials, Surfaces & Interfaces, 3(2), 49–55.
Patel, H. C., Deheri, G. M., & Patel, R. M. H. (2009). Magnetic fluid based squeeze film between porous rough elliptical plates. Journal of Modeling, Design and Management of Engineering Systems, 41, 11–20.
Deheri, G. M., Patel, H. C., & Patel, R. M. H. (2009). Squeeze film between porous elliptical plates. Botswana Journal of Technology, 18(2), 56–63.
Patel, R. M. H., Deheri, G. M., & Vadher, P. A. (2010). Magnetic fluid based squeeze film between annular plates and transverse surface roughness effect. Annals of Faculty of Engineering Hunedoara, 8(1), 51–56.
Vadher, P. A., Deheri, G. M., & Patel, R. M. H. (2010). Performance of hydromagnetic squeeze films between conducting porous rough conical plates. Meccanica, 45(6), 767–783.
Patel, R. M. H., Deheri, G. M., & Vadher, P. A. (2010). Magnetic fluid based short bearing and roughness effects. Journal of Science, 1(1), 102–106.
Patel, R. M. H., Deheri, G. M., & Vadher, P. A. (2010). Performance of a magnetic fluid based squeeze film between transversely rough triangular plates. Tribology in Industry, 32(1), 33–39.
Patel, R. M. H., Deheri, G. M., & Vadher, P. A. (2010). Lubrication of an infinitely long bearing by a magnetic fluid. Fluid Dynamics and Materials Processing, 6(3), 277–290.
Patel, R. M. H., Deheri, G. M., & Patel, H. C. (2010). Effect of transverse surface roughness on circular step bearing. Annals of Faculty of Engineering Hunedoara, 8(2), 23–30.
Patel, R. M. H., Deheri, G. M., & Vadher, P. A. (2010). Performance of a magnetic fluid based short bearing. Acta Polytechnica Hungarica, 7(3), 63–78.
Hayat, T., Qasim, M., & Mesloub, S. (2011). MHD flow and heat transfer over permeable stretching sheet with slip conditions. Int. J. Numer. Meth. Fluids, 66, 963–975.
Deheri, G. M., Patel, H. C., & Patel, R. M. H. (2011). Load carrying capacity and time–height relation. Annals of Faculty of Engineering Hunedoara, 9(1), 33–38.
Patel, R. M. H., Deheri, G. M., & Vadher, P. A. (2011). Magnetic fluid squeeze film between porous plates. Journal of Balkan Tribological Association, 17(2), 305–318.
Deheri, G. M., Patel, R. M. H., & Abhangi, N. D. (2011). Comparative study of magnetic fluid squeeze film. Industrial Lubrication and Tribology, 63(4), 254–270.
Vadher, P. A., Deheri, G. M., & Patel, R. M. H. (2011). Surface roughness effect on conical plates. Journal of Marine Science and Technology, 19(6), 673–680.
Mahantesh, M., Vajravelu, K., Abel, M. S., & Siddalingappa, M. N. (2012). Second order slip flow and heat transfer. Int. J. Thermal Sciences, 58, 142–150.
Patel, R. M. H., Deheri, G. M., & Vadher, P. A. (2012). Rough slider bearing performance. Mathematics Today, 28, 50–62.
Ibrahim, W., & Shankar, B. (2013). MHD nanofluid flow past stretching sheet. Computers & Fluids, 75, 1–10.
Bhattacharyya, K., Hayat, T., & Alsaedi, A. (2013). Casson fluid MHD boundary layer flow. Chinese Physics B, 22.
Mukhopadhyay, S. (2013). Casson fluid flow and heat transfer. Chinese Physics B, 22.
Deheri, G. M., Patel, R. M. H., & Patel, H. C. (2013). Magnetic fluid squeeze film. Journal of Computational Methods, 13, 419–432.
Abou-Zeid, M. Y., Shaaban, A. A., & Alnour, M. Y. (2015). Natural convective effects in porous medium. Journal of Porous Media, 18, 1091–1106.
Patel, H. P., Deheri, G. M., & Patel, R. M. H. (2015). Ferrofluid squeeze film in annular plates. IJSER, 6(8).

Makinde, O. D., Mabood, F., Khan, W. A., & Tshehla, M. S. (2016). Variable viscosity nanofluid flow. Journal of Molecular Liquids, 219, 624–630.
Swain, K., Parida, S. K., & Dash, G. C. (2017). MHD heat and mass transfer. AMSE Modelling B, 86, 706–726.
Ibrahim, S. M., et al. (2017). Chemical reaction in Casson nanofluid. Journal of Engineering Thermophysics, 26, 256–271.
Swain, K., et al. (2018). Non-uniform heat source/sink effects. Defect and Diffusion Forum, 389, 110–127.
Swain, K., et al. (2018). Thermal slip effect. European Journal of Electrical Engineering, 20, 215–233.
Swain, K., et al. (2019). Chemical reaction on MHD nanofluid. Mathematical Modelling of Engineering Problems, 6, 293–299.
Senapati, M., Swain, K., & Parida, S. K. (2020). 3D MHD Casson nanofluid. Karbala Int. Journal of Modern Science, 6.